DMD Fast Forward. Published on January 18, 2022 as DOI: 10.1124/dmd.121.000668
This article has not been copyedited and formatted. The final version may differ from this version.

1. TITLE PAGE

Metabolic Disposition of Lurbinectedin, a Potent Selective Inhibitor of Active Transcription of Protein-Coding Genes, in Nonclinical Species and Patients.

P. Aviles[1*], R. Altares[1], L. van Andel[2†], R. Lubomirov[1], S. Fudio[1], H. Rosing[2], F. M. Márquez del Pino[1], M.M. Tibben[2], G. Benedit[1], L. Nan-Offeringa[2], X.E. Luepke Estefan[1], A. Francesch[1], A. Zeaiter[1], C. Cuevas[1], J.H.M. Schellens[2††]. J.H. Beijnen[2].

Authors´ affiliations:

1. PharmaMar S.A., Colmenar Viejo, Madrid, Spain.
2. Antoni van Leeuwenhoek Hospital, The Netherlands Cancer Institute, Plesmanlaan 121, 1066CX, Amsterdam, The Netherlands.

Current address:

[†]L. van Andel
Toegepast Natuurwetenschappelijk Onderzoek (TNO)
Departement of MHR – team AMS
Zernikedreef 9
2333 CK Leiden
The Netherlands
E-mail: lotte.vanandel@tno.nl

[††]J.H.M. Schellens
Utrecht University
Department of Pharmaceutical Sciences
Universiteitsweg 99
3584 CG Utrecht
E-mail: j.schellens@gmail.com

[*] Corresponding author: Pablo Aviles, PharmD, PhD, ERT, Department of Research and Development, PharmaMar S.A., Avenida de los Reyes 1, Colmenar Viejo 28770, Madrid, Spain.
Phone: +34 918 466 000.
Fax: +34 918 466 001.
E-mail: paviles@pharmamar.com

DMD Fast Forward. Published on January 18, 2022 as DOI: 10.1124/dmd.121.000668
This article has not been copyedited and formatted. The final version may differ from this version.

2. RUNNING TITLE PAGE

ADME of lurbinectedin in nonclinical species and patients.

Corresponding author: Pablo Aviles, PharmD, PhD, ERT. Department of Research and Development, PharmaMar S.A., Avenida de los Reyes 1, Colmenar Viejo 28770, Madrid, Spain.

Phone: +34 918 466 000

Fax: +34 918 466 001

E-mail: paviles@pharmamar.com

Number of text pages: 39

Number of tables: 2

Number of figures: 9

Number of references: 26

Number of words in Abstract: 245

Number of words in Introduction: 363

Number of words in Discussion: 1251

ABBREVIATIONS: *ca.*: *circa*, approximately; vs.: versus

DMD Fast Forward. Published on January 18, 2022 as DOI: 10.1124/dmd.121.000668
This article has not been copyedited and formatted. The final version may differ from this version.

3. ABSTRACT

Lurbinectedin is a novel and potent selective inhibitor of active transcription of protein-coding genes, triggering apoptosis of cancerous cells, which has been approved for the treatment of patients with metastatic small-cell lung cancer with disease progression on or after platinum-based chemotherapy. Different studies aimed at exploring the disposition and metabolism of lurbinectedin were performed in vitro and in vivo (by intravenous administration of lurbinectedin). Low blood cell partitioning for lurbinectedin in rat, nonhuman primate (NHP) and human was determined as 23.4%, 29.8% and 9.8%, respectively. Protein binding was very high (>95%) in total plasma (rat, NHP, human), albumin and α-1-acid glycoprotein (both from human). *In vitro*, lurbinectedin underwent intense liver microsome-mediated metabolism (in 10 minutes, an 80% of the compound is metabolized in human), with CYP3A4 being the isoform involved in that metabolism; results also showed NHP being the nonclinical species which, metabolically, most closely resembles humans. Mass balance studies performed in rats (both genders), NHP (male only) and patients (both genders) demonstrated that the principal route of excretion of ^{14}C-lurbinectedin-related radioactivity was through the feces (88.7±10.1% in patients), with only a minor fraction recovered from the urine (5.6±2.0% in patients). In plasma samples, the majority of lurbinectedin-related radioactivity was attributed to unchanged compound (95±3.1% and 70.2±10.9% in NHP and human, respectively); plasma metabolic profiling demonstrated the major (% compared to unchanged compound) circulating metabolites were *N*-Desmethyl-lurbinectedin (0.4±0.2% and 10.4±2.2% in NHP and patients, respectively) and 1',3'-Desmethylene-lurbinectedin (0.9±0.7% and 14.3±10.4% in NHP and patients, respectively).

DMD Fast Forward. Published on January 18, 2022 as DOI: 10.1124/dmd.121.000668
This article has not been copyedited and formatted. The final version may differ from this version.

4. SIGNIFICANCE STATEMENT

Lurbinectedin is a novel and potent selective inhibitor of active transcription of protein-coding genes, triggering apoptosis of cancerous cells, recently approved for the treatment of patients with metastatic small-cell lung cancer with disease progression on or after platinum-based chemotherapy. The present study provides a complete set of information on the pharmacokinetics, biotransformation and elimination of ^{14}C-lurbinectedin and its metabolites, following a single intravenous administration to nonclinical species (rats and NHP) and patients.

DMD Fast Forward. Published on January 18, 2022 as DOI: 10.1124/dmd.121.000668
This article has not been copyedited and formatted. The final version may differ from this version.

5. INTRODUCTION

Lurbinectedin (1*R*,6'*R*,6a'*R*,7'*R*,13'*S*,14'*S*,16'*R*)-8',14'-dihydroxy-6,9'-dimethoxy-4',10',23'-trimethyl-19'-oxo-2,3,4,6',7',9,12',13',14',16'-decahydro-6a'*H*-spiro[β-carboline-1,20'-[7,13]epimino[6,16](epithiopropanooxymethano)[1,3]dioxolo[7,8]isoquino[3,2-*b*][3]benzazocin]-5'-yl acetate) is a synthetic tetrahydroisoquinoline alkaloid (Fig. 1). Lurbinectedin-induced antitumor activity is the result of a specific inhibition of the transcription, this being produced by the selective binding to CG-rich sequences, mainly those located around promoters of protein-coding genes. This induces an irreversible stalling of elongating RNA Pol II on the DNA template, and its specific degradation by the ubiquitin/proteasome machinery that finally leads to the generation of DNA breaks and, subsequent apoptosis in tumor cells (Santamaria Nunez et al., 2016). In transcriptionally-addicted tumor cells, lurbinectedin causes a detachment of transcription factors from their target promoters, inhibiting the block of its trans-activating activity (Di Giandomenico et al., 2014; Harlow et al., 2016), as well as reducing the tumor-associated macrophages and the inflammatory tumor microenvironment (Cespedes et al., 2016; Belgiovine et al., 2017). Lurbinectedin demonstrated a significant *in vivo* activity in a wide variety of human tumors xenografted in mice (Leal et al., 2010; Vidal et al., 2012; Romano et al., 2013; Cespedes et al., 2016; Harlow et al., 2016; Takahashi et al., 2016), which led to the initiation of the clinical development of lurbinectedin. The results gathered from the first-in-human phase I study, in patients with advanced solid tumors, following the administration as 1-hour intravenous infusion of lurbinectedin every 3 weeks (Elez et al., 2014), demonstrating that myelosuppression (mainly consisting of non-febrile, short lasting, transient grade 4 neutropenia) was the primary toxicity at the recommended dose (4 mg/m^2); other adverse events were fatigue (mild/moderate), nausea and vomiting. Owing to the relevance of the results gathered from a recent clinical trial (Trigo et al., 2020), lurbinectedin has been approved in the USA (https://www.fda.gov/), the United Arab Emirates (https://www.mohap.gov.ae/), Australia (https://www.tga.gov.au/), Singapore (https://www.hsa.gov.sg/) and Canada (https://www.canada.ca/), for the treatment of patients with metastatic small-cell lung cancer (SCLC) with disease progression on or after platinum-based chemotherapy.

DMD Fast Forward. Published on January 18, 2022 as DOI: 10.1124/dmd.121.000668
This article has not been copyedited and formatted. The final version may differ from this version.

This article summarizes the results obtained from a series of *in vitro* and *in vivo* experiments aimed at describing the disposition and metabolism of lurbinectedin in nonclinical species, namely rats and NHP (cynomolgus; *Macaca fascicularis*). The results gathered from an open-label, mass balance clinical trial (including metabolite identification) of lurbinectedin in patients with advanced cancer, are also presented.

DMD Fast Forward. Published on January 18, 2022 as DOI: 10.1124/dmd.121.000668
This article has not been copyedited and formatted. The final version may differ from this version.

6. MATERIAL AND METHODS

Test Articles

Lurbinectedin, as well as reference standards for primary metabolites namely, *N*-Desmethyl-6-Hydroxy-lurbinectedin (Metabolite 1; coded as PM030036), 6-Hydroxy-lurbinectedin (Metabolite 2; coded as PM01158), *N*-Desmethyl-lurbinectedin (Metabolite 6; coded as PM030047), and 14'-Dehydroxy-lurbinectedin (Metabolite 7; coded as PM030779), as well as for the impurity 8',11'-Dioxo-lurbinectedin (coded as PM080323) were synthetized by PharmaMar S.A. (Colmenar Viejo, Spain); the metabolite 1',3'-Desmethylene-lurbinectedin (or Metabolite 4) was obtained by the method described elsewhere (Altares et al., 2019). ^{14}C-lurbinectedin (specific activity, 54 μCi/mg; radiochemical purity, 92.2%, coded as PM100567) labeled at substituted C4 indole (Fig. 1), which was proven to be metabolically stable (both, *in vitro* and *in vivo*) was also synthetized by PharmaMar S.A., as well as the deuterated lurbinectedin (Fig. 1) (coded as PM040038) that was used as the bioanalytical internal standard.

Chemical and Reagents

Human and rat plasma were purchased from Sera Laboratories, Ltd. (Sussex, UK); NHP plasma was obtained from the animal science laboratory at Aptuit (Verona, Italy). Human albumin and α-1-acid glycoprotein were purchased from Sigma-Aldrich (St. Louis, MO, USA). Rat, NHP and human blood were sourced from Aptuit (Verona, Italy). For the *in vitro* metabolism experiments, pooled batches of rat, NHP and human liver microsomes were obtained from Xenotech (Kansas City, KS, USA); pooled human liver microsomes (BD Biosciences; San Jose, CA, USA), as well as CYP2B6 and CYP2C19) supersomes™ (Corning Inc.; NY, USA) were used for the identification, by specific chemical inhibition, of the cytochrome P450 isoforms involved in the oxidative metabolism of lurbinectedin. The specific chemical inhibitors used in these experiments were obtained either from Merck KGaA (Darmstadt, Germany): furafylline, 8-methoxypsoralen, sulfaphenazole, quinidine, diethyldithiocarbamate, ketoconazole, montelukast; or, from Cypex Ltd. (Dundee, Scotland, UK): 3-benzyl-phenobarbital; or, from TargetMol (Boston, MA, USA): sertraline. The CYP-specific chemical substrates used were verapamil, phenacetin, coumarin, diclofenac, omeprazole, dextromethophan, chlorzoxazone, testosterone, paclitaxel, midazolam (all from Merck KGaA; Darmstadt, Germany) and, efavirenz (TargetMol®; Wellesley Hills, MA, USA). Glucose-6-

DMD Fast Forward. Published on January 18, 2022 as DOI: 10.1124/dmd.121.000668
This article has not been copyedited and formatted. The final version may differ from this version.

phosphate dehydrogenase, glucose-6-phosphate and NADP were provided by Corning Inc. (NY, USA). All other chemicals were reagent grade unless otherwise stated.

Blood Cell Partitioning Determination

Five milliliters of rat, NHP or human whole blood (all collected with K_3EDTA as anticoagulant) were spiked with ^{14}C-lurbinectedin to reach a final concentration of 200 and 500 nM (157 and 393 ng/mL, respectively; 1 nM=0.79 ng/mL). Following 15 minutes of equilibration time at 37ºC, samples were centrifuged at 2000xg for 10 minutes at 5ºC and then, 2 aliquots were taken (250 µL each). The first aliquot was centrifuged to obtain plasma; the second, was solubilized by Solvable™ (Perkin Elmer, Waltham, MA, USA), added with 30% hydrogen peroxide and incubated for at least 2 hours at approximately 50ºC. Then, both solubilized blood and plasma was assayed for radioactivity as described below. Before and after incubation, blood was collected into glass capillaries and hematocrit (Hto) determined by centrifuging 15000xg for 10 minutes. Blood cell partitioning (BCP, %) was determined by applying the following equation:

$$\%BCP = \left[1 - \frac{C_p \times (1 - Hto)}{C_b}\right] x100$$

Where C_p and C_b was lurbinectedin concentration in plasma and blood, respectively. Each experiment was carried out in triplicate. Details on the determination of equilibration time, as well as compound stability in whole blood are not described in this article.

Plasma Protein, Albumin and α-1-Acid Glycoprotein Binding

Rat and NHP (male only) plasma, as well as human (pooled genders) plasma, and human albumin (50 and 25 mg/mL) and α-1-acid glycoprotein (1.5 and 0.5 mg/mL) were fortified with lurbinectedin to reach a final concentration of 500, 200, 50 and 10 nM (392, 157, 39.2 and 7.8 ng/mL, respectively). Solutions were gently mixed for 15 minutes at 25ºC to equilibrate prior to ultrafiltration. Samples were transferred to Centrifree® ultrafiltration devices with Ultracel® regenerated cellulose membrane (30 KDa) (Merck KGaA; Darmstadt, Germany), centrifuged (1500xg at 25ºC) for either 5 minutes (albumin and α-1-acid glycoprotein) or 15 minutes (plasma) and then, retained and ultrafiltrated fluids were analyzed by LC-MS/MS for lurbinectedin concentration

DMD Fast Forward. Published on January 18, 2022 as DOI: 10.1124/dmd.121.000668
This article has not been copyedited and formatted. The final version may differ from this version.

(see below Method 1). The binding (B, %) of lurbinectedin to proteins was determined by using the equation:

$$\%B = 1 - \frac{C_u}{C_o} \times 100$$

Where C_0 and C_u was the concentration of lurbinectedin at t=0 minutes and in the ultra-filtrate, respectively. Each experiment was done in triplicate.

***In vitro* Microsome Incubations and Metabolic Profiling**

Incubations of either ^{14}C-lurbinectedin or lurbinectedin with liver microsomes from rat and NHP (both genders), as well as from human (pooled both genders), were carried out at a protein concentration of 0.5 mg/mL in a total volume of 1 mL. The co-factor mixture in each incubate contained 3.3 mM of glucose-6-phosphate, 0.4 U/mL units of glucose-6-phosphate dehydrogenase, 3.3 mM of $MgCl_2$ and 1.3 mM of $NADP^+$ in 1.0 mL of a 0.1 M potassium phosphate buffer pH 7.4 (Corning Inc., NY, USA). Lurbinectedin or ^{14}C-lurbinectedin solutions were prepared to give a final concentration of 400 nM (314 ng/mL) in 1 mL of enzymatic reaction. After 5 minutes of the pre-incubation phase, the reaction was started with the addition of the NADPH regenerating system, according to the supplier`s instructions (BD Biosciences, San Jose, CA, USA). Reaction was incubated for 10 minutes at 37ºC under continuous shaking. Following each incubation (replicated 10 times per species and gender) with activated microsomes, the enzymatic reaction was stopped by adding 1 mL of cold acetone with 0.1% formic acid (1:1, v:v) and then, the mixture was centrifuged (15500xg at room temperature). Radioactivity was determined in the pellet and in 100 µL aliquot from the supernatant. Another 100 µL aliquot from the supernatant was injected into the HPLC system (see below Method 2). Column eluting fractions were collected and the recovered radioactivity was determined in the column eluent that was collected into 100 different fractions (15 seconds each; cumulative collection in the same vial coded as F1 to F100), using a 1260 Infinity Fraction Collector AS (Agilent Technologies, Inc., Santa Clara, CA, USA). This procedure was repeated in each incubation, collecting each fraction in the same vial. After mixing with 5 mL of scintillation liquid (Ultima-FLO M; Perkin-Elmer, Waltham, MA, USA), the radioactivity was measured by a scintillation liquid counter (Hidex 300 SL; Hidex, Turku, Finland). The value of radioactivity (dpm) obtained in each fraction was plotted vs. time (minutes) and then, a radiochemical chromatogram was constructed for each species evaluated. In these radiochemical

DMD Fast Forward. Published on January 18, 2022 as DOI: 10.1124/dmd.121.000668
This article has not been copyedited and formatted. The final version may differ from this version.

chromatograms, any fraction with radioactivity values 2-fold higher than the corresponding fraction in the blank solvent was considered for further calculations.

Chemical Inhibition of Cytochrome P450 Activities

Lurbinectedin (200 nM; 157 ng/mL) was incubated (in triplicate) at 37ºC in NADPH-activated human liver (protein concentration, 0.5 mg/mL) microsomes or supersomes™ with CYP-selective chemical inhibitors: furafylline 10 μM (CYP1A2); 8-methoxypsoralen 10 μM (CYP2A6); sertraline 100 μM (CYP2B6); montelukast 10 μM (CYP2C8); sulfaphenazole 10 μM (CYP2C9); phenobarbital 10 μM (CYP2C19); quinidine 3 μM (CYP2D6); diethyldithiocarbamate 100 μM (CYP2E1); and, ketoconazole 10 μM (CYP3A4). At different time points (0, 5, 10, 15, 20 and 25 minutes) an aliquot (100 μL) of the incubation mixture was added to cold acetone 0.1% with formic acid (100 μL), centrifuged (10000xg at 5ºC for 10 minutes) and, the resulting supernatant subjected to LC-MS/MS analysis (see below Method 3). Blank control (lurbinectedin incubation without NADPH) and blank reagent (incubation with NADPH, without lurbinectedin) were included as a control in each replicated incubation.

Mass Balance Experiments

All animal protocols were reviewed and approved according to regional Institutional Animal Care and Use Committees. Animals (rat or NHP) received a single intravenous bolus administration of ^{14}C-lurbinectedin at the maximum tolerated dose, which was determined in separate experiments that are not detailed in this article. Sprague-Dawley rats (approximately 7 to 9 weeks of age) were purchased from Charles River (Milano, Italy), whereas NHP (approximately 4.5 years old) were obtained from LCL-Cynologics IBL House (Port Louis, Mauritius) and quarantined at SILABE ADUEIS (Strasburg, France).

The open-label, mass balance clinical trial of lurbinectedin in patients with advanced cancer was conducted in conformance with the International Conference on Harmonization guidelines for Good Clinical Practice and in accordance with the Declaration of Helsinki. The protocol was approved by the Netherlands Cancer Institute Independent Ethics Committee. All patients signed the written informed consent before they were enrolled in the clinical trial.

DMD Fast Forward. Published on January 18, 2022 as DOI: 10.1124/dmd.121.000668
This article has not been copyedited and formatted. The final version may differ from this version.

Mass balance in rats.

Sprague-Dawley rats (*N*=27/gender) were intravenously administered at 1.2 mg/m^2 (11.2 μCi/kg; male) and 0.6 mg/m^2 (5.6 μCi/kg; female) of ^{14}C-lurbinectedin (the maximum tolerated dose in male and female, respectively) and placed in stainless steel metabolic cages. After 0.25, 0.5, 1, 2, 4, 8, 24, 48 and 72 hours of compound administration, blood samples were collected (*N*=3/gender) in K_3EDTA containing tubes from the abdominal aorta of euthanized animals. In a separate experiment, additional animals (*N*=3/gender) were dosed with the compound (at the same dose levels) and then, refrigerated urine (intervals: 0-8, 8-24 hours and then, daily) and feces (daily) were collected for a period of 7 days; residual radioactivity in body carcasses was determined at the end of the experimental period. Also, the biliary excretion of ^{14}C-lurbinectedin-related material was studied separately. Bile duct cannulated Sprague-Dawley rats (*N*=3/gender) were treated at the same dose levels and their bile was then collected at 0-8, 8-24, 24-48 and 48-72 hours post-administration; feces and carcasses were also sampled at the end of the experiment (72 hours). Residual radioactivity was measured by daily rinsing with ethanol:water (1:1, v:v) of the metabolic cages and by washing with an aqueous solution of Radiacwash™ (Nukepills Inc.; Edgewater, MD, USA) at the end of collection period (168 hours). Mixtures of feces and ultrapure water (1:1.5, w:v) were homogenized (Precellys 24 Dual; Bertin Instruments, Montigny-le-Bretonneux, France) and then, weighed homogenates were mixed with Solvable™ (Perkin-Elmer; Waltham, MA, USA), 30% hydrogen peroxide, isopropyl alcohol and incubated 2 hours at 50ºC. Animal carcasses were solubilized with a solution of 40% KOH in methanol (w:v) and, further mixed with 30% hydrogen peroxide. Radioactivity was measured in fecal homogenates (4/sampling time), solubilized carcasses (*N*=4/sample) and in original liquid samples (namely, urine, bile, plasma, cage rinse; *N*=2/sample).

Mass balance in NHP.

Three non-naïve, male NHP were dosed at 1.7 mg/m^2 (9.4 μCi/kg) of ^{14}C-lurbinectedin by intravenous route and then, housed in metabolic cages. At selected time points (0.08, 0.25, 0.5, 1, 2, 4, 8, 24, 48, 72, 96, 120 and 144 hours) post-dosing, animals were sampled from the cephalic/femoral vein or the femoral artery, and blood collected in K_3EDTA containing tubes and divided into 2 aliquots: the first (blood) was kept at 5ºC; the second aliquot was centrifuged and plasma obtained and divided into 2 aliquots,

DMD Fast Forward. Published on January 18, 2022 as DOI: 10.1124/dmd.121.000668
This article has not been copyedited and formatted. The final version may differ from this version.

which were stored at -80ºC until further analysis. In the first aliquot, ^{14}C-lurbinectedin-related total radioactivity was determined by liquid scintillation counting; the second plasma aliquot was precipitated by adding (1:3, v:v) of cold acetone 0.1% formic acid and then, supernatants were analyzed by LC-MS/MS (see below Method 3) to identify the parent compound and its main metabolites. Protein pellets and the three consecutive rinses were counted by liquid scintillation counting for residual ^{14}C-lurbinectedin-related radioactivity retained in plasma proteins.

Urine was collected, refrigerated at intervals of 0-8, 8-24, 24-48, 48-72, 72-96, 96-120, 120-144 and 144-168 hours after compound administration; feces were collected daily up to 7 days post-dosing and weights recorded. Daily, metabolic cages were rinsed with ethanol/water (1:1; v:v) and washed with an aqueous Radiacwash™ (Nukepills Inc.; Edgewater, MD, USA) solution at the end of the collection period (168 hours).

Feces samples were homogenized with ultrapure water (1:1; w:v). Further, weighed aliquots (4/sampling time) of homogenates were solubilized by Solvable™ (Perkin-Elmer; Waltham, MA, USA) and 30% hydrogen peroxide for 2 hours at 50ºC; blood samples were treated so. All samples were then counted for radioactivity as described below.

Mass balance in patients.

Six patients with advanced cancer (namely, oropharynx carcinoma, melanoma, pancreatic adenocarcinoma, breast cancer, neuroendocrine carcinoma and cancer of unknown primary origin) were enrolled in a phase I, open-label, uncontrolled study to characterize the mass balance following a single administration of ^{14}C-lurbinectedin as 1-hour intravenous infusion at 5 mg (flat dose). The median age (range) of patients was 59 (52-68) years. Infusion bags were prepared by PRA Health Sciences (Groningen, the Netherlands) by adding the appropriate amounts of ^{14}C-lurbinectedin and non-radiolabeled lurbinectedin to give a final solution containing exactly 5.0 mg of lurbinectedin, with 100 μCi of radioactivity, in 124 mL of sodium chloride (0.9%). Infusion bags were weighed before and after drug infusion and then, the exact dose (^{14}C-lurbinectedin and non-radiolabeled lurbinectedin) administered to each patient was calculated; subsequent doses of lurbinectedin were prepared with non-radiolabeled compound at a dose of 3.2 mg/m^2. Venous blood samples (from the contralateral arm to intravenous infusion) were collected in Vacutainer® K_3EDTA tubes (Becton, Dickinson

DMD Fast Forward. Published on January 18, 2022 as DOI: 10.1124/dmd.121.000668
This article has not been copyedited and formatted. The final version may differ from this version.

and Company; Franklin Lakes, NJ, USA) at the following time points: pre-dosed, just before the end of infusion (EOI), 0.08, 0.25, 1, 1.5, 2, 4, 6, 8, 10, 12 hours and, on the morning of days 2 to 8. Feces were collected until less than 1% of the administered radioactive dose was excreted over 24 hours for two consecutive days (cessation criteria) and, urine at pre-dose, and during the following intervals 0-12, 12-24 hours and then, daily until the cessation criteria was met. Blood samples were aliquoted (2 x 200 µL each) and added with Solvable™ (Perkin-Elmer, Waltham, MA, USA), 30% hydrogen peroxide, NaEDTA and incubated approximately at 40 ºC until samples became translucent; the remaining blood, was centrifuged and the plasma obtained was used for total radioactivity counting determination. Feces samples were digested by incubating (until transparency reached) a mix with Solvable™ (Perkin-Elmer, Waltham, MA, USA), 30% hydrogen peroxide and isopropyl alcohol at 40 ºC. Plasma and urine samples were counted for total radioactivity without performing any previous treatment. Metabolic profiling was evaluated in plasma, feces and urine samples frozen at -70 ºC until LC-MS/MS (see below Method 4) analysis was carried out.

Determination of Total Radioactivity

Aliquots of samples (weighed fecal homogenates, solubilized animal carcasses, as well as original liquid samples, such as urine, blood, plasma or cage rinses) were added with an appropriate volume of scintillation cocktail (Ultima Gold™; Perkin-Elmer, Waltham, MA, USA) and then, total radioactivity was measured by liquid scintillation counting using Tri-Carb® 2900 TR liquid scintillation spectrometer (Perkin-Elmer, Waltham, MA, USA).

LC-MS/MS Methods

Four LC-MS/MS methods were used throughout these experiments. The first method was used in the quantitation of lurbinectedin in samples from *in vitro* studies of binding to plasma protein, albumin and α-1-acid glycoprotein; the second method, was used for the quantitation of lurbinectedin and metabolic profiling in samples from both *in vitro* and *in vivo* studies (NHP); whereas the third method, was dedicated to the quantitation of lurbinectedin in samples obtained from the *in vitro* chemical inhibition of Cytochrome P450. Lurbinectedin and its metabolites in patient-derived samples were quantified by applying the fourth LC-MS/MS method. In all samples obtained from both NHP and patients, the quantitation of the compounds was accomplished by using

DMD Fast Forward. Published on January 18, 2022 as DOI: 10.1124/dmd.121.000668
This article has not been copyedited and formatted. The final version may differ from this version.

the corresponding MS/MS transitions obtained for lurbinectedin and/or ^{14}C-lurbinectedin and its related metabolites.

Method 1 (used for lurbinectedin analysis in in vitro studies of plasma binding to protein, albumin and α-1-acid glycoprotein).

Lurbinectedin was analyzed in samples already prepared by adding cold acetone with 0.1% formic acid (1:1, v:v) and then, centrifuged. Lurbinectedin was separated on a 2.1x50 mm column, packed with 1.7 µm BEH Phenyl (Acquity; Waters, Milford, MA, USA) and kept at 45 ºC. Chromatography (Acquity UPLC; Waters, Milford, MA, USA) was carried out (at a flow rate of 0.7 mL/min) with 0.1% formic acid in 10 mM ammonium formate (A) and acetonitrile (B) using isocratic conditions (A:B; 60:40, v/v). Detection was done by tandem mass spectrometry (Sciex API5000; AB SCIEX, Framingham, MA, USA) operated in the positive mode. Multiple reaction monitoring was used for quantification.

Method 2 (used for the quantitation of lurbinectedin and metabolic profiling in microsomes incubations and plasma samples from NHP).

Samples were prepared by adding (1:1, v:v in microsomes; 1:3, v:v in plasma) cold acetone with 0.1% formic acid and then, centrifuged. Supernatants were subjected to a gradient phase chromatography, in which analytes (lurbinectedin and its metabolites) were separated on an ACE C18 PFP, 3 µm, and 2.1x150 mm column (Advanced Chromatography Technologies, Aberleen, UK) heated to 50ºC. Liquid chromatography (Agilent 1290 infinity; Agilent Technologies, Inc., Santa Clara, CA, USA) was carried out at a flow rate of 0.4 mL/min using a gradient of water (A) in acetonitrile (B), both with 0.1% formic acid: 90 to 70% A from 0.0 to 12.0 minute; 70 to 30% A from 12.0 to 18.0 minute; 30 to 10% A from 18.0 to 20.0 minute; isocratic for 1.0 minute and then, returning to initial conditions in 0.1 minute, kept isocratic up to the minute 25.0. Relevant information on MS/MS fragmentation of lurbinectedin is presented in Fig 3.

Method 3 (used for quantitation of lurbinectedin in vitro chemical inhibition of cytochrome P450).

Lurbinectedin was analyzed in samples already prepared by adding cold acetone with 0.1% formic acid (1:1, v:v) and then, centrifuged. Lurbinectedin was separated on a 2.1x30 mm column, packed with 3 µm ACE C18 PFP (Advanced Chromatography Technologies, Aberleen, UK) and kept at 50ºC. Gradient chromatography (Agilent 1290

DMD Fast Forward. Published on January 18, 2022 as DOI: 10.1124/dmd.121.000668
This article has not been copyedited and formatted. The final version may differ from this version.

infinity; Agilent Technologies, Inc., Santa Clara, CA. USA) was carried out (at a flow rate of 0.6 mL/min) using 0.1% formic acid in water (A) and 0.1% formic acid in acetonitrile (B) with the following profile: gradient to 90% to 10% A from 0. 0 to 2.5 minute; isocratic 10 % A from 2.5 to 3.5 minute; and then, initial conditions during 1.5 minutes. Detection was by tandem mass spectrometry (API4000 or API4500 QTrap; AB SCIEX; Framingham, MA, USA) operated in the positive mode. Multiple reaction monitoring was used for quantification.

Method 4 (used for the quantitation of lurbinectedin and its metabolites in plasma and urine samples obtained in the clinical trial in patients).

A previously described method used for the quantification of lurbinectedin in human plasma and urine (van Andel et al., 2018) was modified to optimize the analysis of lurbinectedin-related metabolites (Method B). In short, 100 µL of plasma samples and 10 µL of urine diluted with 90 µL control human K_3EDTA plasma (to prevent adsorption of the drug to the tubes) were pretreated with TBME. Samples were dried by gentle N_2 stream (at 25ºC) and dried extracts were resuspended in 0.1% formic acid in water:acetonitrile (70:30; v:v). Liquid chromatography (UPLC Acquity I class; Waters, Milford, MA, USA) was done on a 150x2.1 mm column, packed with Zorbax-SB C18, 5 µm, (Agilent Technologies, Inc. Santa Clara, CA, USA) and kept at a temperature of 50ºC. The mobile phase was a mixture of A: 0.1% formic acid in water: acetonitrile (90:10; v:v); and, B: 0.1% formic acid in acetonitrile:water (90:10; v:v). The flow was 0.4 mL/min. Following an isocratic period of 1 minute (A/B; 100/0), a gradient was used from (A/B; 100/0) to (A/B; 83/17) over 31 minutes, then to (A/B; 0/100) in 0.1 minute, kept until 34 minutes and back to initial conditions in 0.1 minute; column was then re-conditioned for 3 minutes. Detection was performed by tandem mass spectrometry (Sciex API5500 Q-Trap; AB SCIEX, Framingham, MA, USA) with turbo ion spray, operated in the positive ion mode.

Control human plasma and urine were spiked with lurbinectedin to prepare calibration standards (8 concentration levels from 0.1 to 100 ng/mL) and quality control (QC) samples (at 0.3, 3 and 75 ng/mL). Separate calibration standards and QC samples were spiked for the metabolites in plasma (range from 0.1 to 25 ng/mL) and in urine (range from 1 to 250 ng/mL). The linear regression of the peak area ratio vs. the concentration was weighted by $1/\chi^2$ (the reciprocal of the squared concentration). For every calibration standard, the concentrations were back-calculated from the responses. At least 75% of

DMD Fast Forward. Published on January 18, 2022 as DOI: 10.1124/dmd.121.000668
This article has not been copyedited and formatted. The final version may differ from this version.

the non-zero standards were within ±15% of the actual value (or ±20% for the lower limit of quantification) and at least 50% of the QC samples at each concentration level and 2/3 of all QC samples were within ±15% of the nominal concentration for each analytical run, hence adequate assay performance in terms of intra- and inter-assay accuracy and precision was demonstrated.

In order to allow the direct comparison between the concentrations calculated from the total radioactivity counting, metabolite calculated concentrations were converted into the ng-equivalent (eq)/mL of lurbinectedin by multiplying the concentration of the given metabolite by the molecular weight ratio of the metabolite and lurbinectedin.

Structural Elucidation of Metabolites

The structure of lurbinectedin-related metabolites found in either *in vitro* or *in vivo* experiments was elucidated on the basis of molecular mass, charged molecular ions and collision-induced dissociation fragments (Oliveira and Watson, 2000). All the structures of the proposed lurbinectedin-related metabolites were fully confirmed by comparison of chromatography retention times and fragmentation patterns obtained with authentic synthetic standards, which were subjected to ^{1}H NMR structural elucidation (with the exception of 1',3'-Desmethylene-lurbinectedin; Metabolite 4).

Data Analysis

The total radioactivity excreted in urine, bile and feces was expressed as the percentage of the given radioactivity. Individual plasma concentrations at nominal sampling times were used to assess pharmacokinetic parameters using standard non-compartmental methods via the WinNonlin® 6.3 Phoenix®64 software (Pharsight Co., Saint Louis, MO, USA). Results were presented as mean±SD, unless otherwise specified. Statistical analyses (2-tailed Mann–Whitney *U* test) were done and graphs plotted using GraphPad Prism, version 9.2.0 (GraphPad Software, San Diego, CA, USA).

DMD Fast Forward. Published on January 18, 2022 as DOI: 10.1124/dmd.121.000668
This article has not been copyedited and formatted. The final version may differ from this version.

7. RESULTS

Blood Cell Partitioning

The blood cell partitioning in rat, NHP and human was determined by spiking whole blood with ^{14}C-lurbinectedin to reach a final concentration of 200 and 500 nM (157 and 393 ng/mL, respectively). Regardless of the concentration assayed, low values for blood cell partitioning were determined for rats (23.2 to 23.6%), NHP (29.7 to 29.8%) and human (9.5 to 10.6%), these values being in agreement with the lack of compound distribution (evaluated as lurbinectedin-related-radioactivity) into blood cells determined in the *in vivo* studies carried out either in nonclinical species (rat and NHP) or patients.

Plasma Protein, Albumin and α-1-Acid Glycoprotein Binding

The binding to plasma proteins was studied by LC-MS/MS analysis of lurbinectedin-fortified, ultrafiltrated plasma at 10, 50, 200 and 500 nM (7.8, 39.2, 157 and 392 ng/mL, respectively) from rat, NHP and human. Regardless of either the species examined or the concentration of lurbinectedin, a very high percentage of binding to proteins of plasma from rat, NHP and human was found (>95%). Lurbinectedin (at identical concentrations as above) displayed a very high percentage of binding to physiological concentrations of specific human-obtained proteins, namely albumin (50 and 25 mg/mL) and α-1-acid glycoprotein (1.5 and 0.5 mg/mL).

In vitro Microsome-Mediated Lurbinectedin Metabolism, Metabolism Profiling and Cytochrome P450 Isoforms Involved

Incubations (at 37ºC) of ^{14}C-lurbinectedin (400 nM; 315 ng/mL; 0.02 μCi) with rat-, NHP- or human-derived liver microsomes (0.5 mg/mL of protein) in the presence of NADPH-regenerating were kept for 10 minutes, stopped by the addition of cold acetone (with 0.1% of formic acid) and then centrifuged. In supernatants, recovered radioactivity ranged from 82% (rat, female) to 88% (rat, male; human, pooled); resulting pellets retained between 13% (rat, male) and 23% (NHP, male) of the initially incubated ^{14}C-lurbinectedin-related radioactivity. After the incubation period, ^{14}C-lurbinectedin was nearly or even completely metabolized (% remaining unchanged) by liver microsomes from NHP (5.9±0.1 and 5.2±1.2 male and female, respectively;

DMD Fast Forward. Published on January 18, 2022 as DOI: 10.1124/dmd.121.000668
This article has not been copyedited and formatted. The final version may differ from this version.

N=3/gender), human (17.8±5.8 pooled-both-genders) and, to a lesser extent, rat (65.1±8.9 and 76.9±11.6 male and female, respectively; *N*=3/gender).

Thus, supernatants (100 µL) obtained from 10 independent incubations (triplicated per species and gender) of ^{14}C-lurbinectedin with microsomes were subjected to HPLC separation by using chromatographic Method 3 (see above). Each of the 100 column eluting fractions (15 sec each) was accumulatively collected in the same vial (coded as F1 to F100) and then, counted for radioactivity content. Reconstructed radiochemical chromatograms (counts/fraction vs. time) obtained for each microsomal incubation per gender and species are displayed in Fig. 2, which strongly suggest that NHP and human have the most qualitatively and quantitatively similar microsome-mediated metabolism of ^{14}C-lurbinectedin. The corresponding integration of these reconstructed radiochemical chromatograms are summarized in Table 1. Results suggest a relationship between the total post-column recovery and the metabolic rate, which may be explained by an apparent lack of radioactivity within the small, non-integrable peaks, likely belonging to redundant metabolites. Two main ^{14}C-lurbinectedin-related metabolites were identified and coded as Metabolite 4 and Metabolite 6, the last being found in a similar amount, regardless of the species or gender assayed. However, Metabolite 4 was by far, the more abundant in NHP and human than in rats; two other low-intensity peaks were exclusively found in NHP and human and coded as Metabolite 1 and Metabolite 2. Altogether, these results demonstrated the evident metabolic dissimilarities between rodent and non-rodent (NHP and human) species. The structures of these lurbinectedin-related metabolites were confirmed by the analysis of fragmentation patterns obtained with standards, as well as by the comparison of retention times following the chromatography of those standards.

The mass spectrum of Metabolite 6 revealed a protonated molecular ion at *m/z* 771.5, corresponding to a 14 amu shift relative to lurbinectedin (*m/z* 785.3; Fig. 3); the same 14 amu shift was noticed in the specific protonated molecular ion MS/MS fragment, *m/z* 479.2 (Fig. 4). The chromatography of PM030047 confirmed that Metabolite 6 is the result of *N*-Desmethylation at 23' position in the lurbinectedin structure (Fig. 5). The metabolite coded as Metabolite 4 (*m/z* 773.1) was shifted 12 amu as compared to lurbinectedin (Fig. 3), as well as the protonated molecular ion MS/MS specific fragments (*m/z* 481.1 vs. 493.0, respectively; Fig. 4). The chromatography of the biologically obtained standard demonstrated that Metabolite 4 is 1',3'-Desmethylene-

DMD Fast Forward. Published on January 18, 2022 as DOI: 10.1124/dmd.121.000668
This article has not been copyedited and formatted. The final version may differ from this version.

lurbinectedin, as a result of the aliphatic ring opening at 1' and 3' position of the parent compound (Fig. 5). There were two other minor peaks identified as lurbinectedin-related metabolites, namely Metabolite 2 and Metabolite 1 (Table 1). The protonated molecular ion MS/MS specific fragment of M2 (*m/z* 259.1; Fig. 4) corresponds to a 14 amu shift relative to the equivalent specific fragment of lurbinectedin (*m/z* 273.1; Fig. 4), suggesting thus the lack of a methyl group as the more likely metabolic change produce in lurbinectedin; HPLC analysis of PM01158 confirmed Metabolite 2 as the *O*-Desmethylated lurbinectedin (6-Hydroxy lurbinectedin; Fig. 5). The protonated molecular ion of Metabolite 1 had lost 28 amu (*m/z* 757.3; Fig. 4) compared to lurbinectedin, and the MS/MS specific fragments (*m/z* 259.1 and 479.2; Fig. 4), as well as the HPLC of the compound PM030036, strongly suggest that this metabolite is the result of a di-Desmethylation, leading to *N*-Desmethyl-6-Hydroxy-lurbinectedin (Fig. 5). The other two minor compounds coded as Metabolite 3 and Metabolite 5, were identified as the aliphatic ring opening and the oxidation of Metabolite 6 (data not shown), respectively (Table 1). Therefore, these two compounds, rather than true lurbinectedin metabolites, were likely to be the result of an artifact, owing to the very intensive *in vitro* metabolism, which might produce a metabolite-of-metabolite (redundant *in vitro* metabolism).

As a summary, a proposal for the *in vitro* metabolic pathway of lurbinectedin in NADPH-activated liver microsomes is depicted in Fig. 5. Lurbinectedin was metabolized via several biotransformation pathways including *N*-Desmethylation and/or aliphatic ring opening and/or *O*-Desmethylation.

To identify the specific cytochrome P450 isoforms involved in its metabolism, lurbinectedin (at 200 nM; 157 ng/mL) was incubated with pooled human liver microsomes in the presence of cytochrome P450-selective chemical inhibitors. The disappearance of lurbinectedin as a function of incubation time in the absence and presence of cytochrome P450-isoform selective chemical inhibitors is displayed in Fig. 6. Following a 20-minutes incubation period with pooled human liver microsomes, only a 2.0±0.1% of lurbinectedin remained unchanged. The selective chemical inhibition of the different cytochrome P450-isoforms resulted in residual (mean±SD; *N*=3) lurbinectedin percentages of 2.0±0.4% (CYP1A2), 3.0±1.0% (CYP2A6 and CYP2C9), 5±1.0% (CYP2C8), 2.0±1.0% (CYP2C19), 2.0±0.3 (CYP2D6), 2.0±0.5 (CYP2E1), and 99.0±4.0 (CYP3A4/5). After a 20-minute incubation in Supersomes™, results

DMD Fast Forward. Published on January 18, 2022 as DOI: 10.1124/dmd.121.000668
This article has not been copyedited and formatted. The final version may differ from this version.

demonstrated the lack of CYP2B6 and CYP2C19 mediated metabolism. As such, the percentage (median) of unchanged lurbinectedin was 87% and 71% (*P*=0.100; CYP2B6) and 96% and 86% (*P*=0.300; CYP2C19) without and with chemical inhibition of each isoform, respectively. Results demonstrated that the metabolism of lurbinectedin was completely abolished by ketoconazole, a selective chemical CYP3A4 inhibitor, this isoform being considered, therefore, as the single responsible of lurbinectedin metabolism.

Mass Balance in Rats

A mass balance study was performed, in which Sprague-Dawley rats received a single intravenous bolus dose of ^{14}C-lurbinectedin at 1.2 mg/m^2 (male) and 0.6 mg/m^2 (female). Blood samples were collected (*N*=3/gender) at 0.25, 0.5, 1, 2, 4, 8, 24, 48 and 72 hours post-dose. In another experiment, additional animals (*N*=3/gender) were dosed with the compound, urine and feces collected for a period of 7 days, and then the carcass analyzed for residual radioactivity. Also, the biliary excretion of lurbinectedin-related material was studied separately. Bile duct cannulated Sprague-Dawley rats (*N*=3/gender) were treated at the same dose levels and their bile was then collected up to 72 hours post-administration. The multi-compartment distribution of the concentration-time curves in blood and plasma were similar in both genders, with C_{max} values (64.2 and 33.0 ng-eq/g in blood of male and female, respectively) obtained at 0.25 hours post-dose (Fig. 7). Although males were treated at a higher dose (2-fold) than females, similar systemic exposure to total lurbinectedin-related radioactivity (AUC_{0-t}) was obtained in both genders (340 and 235 ng-eq·h/g in male and female, respectively). The combined recovery of radioactivity in carcass and excreta was about 99%. The data indicated that in rats, the excretion of radioactivity was quick, with the 3% (male) and 6% (female) of radioactivity recovered from the carcass at 7 days post-dose. In this species, the principal route of excretion was through the feces (91.0±2.1% and 91.2±1.7% of total radioactivity in male and female, respectively; *N*=3/gender), with only a minor fraction recovered from the urine (3.4±1.4% in male and 2.6±0.5% in female; *N*=3/gender). From these data, no gender differences were recorded (Table 2).

Mass Balance in NHP

After administration, the maximum levels of ^{14}C-lurbinectedin-related total radioactivity were observed at the first sampling time (0.08 hours), declining rapidly, followed by a

DMD Fast Forward. Published on January 18, 2022 as DOI: 10.1124/dmd.121.000668
This article has not been copyedited and formatted. The final version may differ from this version.

more gradual decrease. This curve shape suggests multi-compartmental kinetics of ^{14}C-lurbinectedin-related radioactivity in male NHP, with no meaningful differences being observed between plasma and blood (Fig. 7). Regardless of the sampling time, results showed similar blood-to-plasma ratio (range, 0.9 to 1.3) of ^{14}C-lurbinectedin-related radioactivity, this being consistent with the values obtained following the *in vitro* evaluation of the blood distribution of lurbinectedin. The main pharmacokinetic parameters (blood vs. plasma; *N*=3/matrix) of ^{14}C-lurbinectedin-related radioactivity in male NHP following a single intravenous bolus dose (1.7 mg/m^2) were: C_{max} (ng-eq/g), 156±74 vs. 159±72; $AUC_{0-\infty}$ (ng-eq·h/mL), 956±164 vs. 888±133; $t_{1/2}$ (h), 77±8 vs. 94±2; CL (L/h/kg), 0.15±0.03 vs. 0.16±0.03; and, Vd_{ss} (L/kg), 12.5±1.7 vs. 16.3±2.2.

The combined recovery of radioactivity in this study (feces, urine and cage rinse) was 82.0±3.1% (*N*=3) (Fig. 8). These data indicated that in NHP the principal route of lurbinectedin`s excretion was through the feces, with cumulative (0 to 168 hours post-dose) radioactivity excretion determined as 75.9±0.9% (*N*=3) of the dose administered; only a minor fraction of the ^{14}C-lurbinectedin-related radioactivity was recovered from the urine (4.0±1.1%; *N*=3).

Plasma samples obtained in the study were subjected to further analysis, in which lurbinectedin and its metabolites were quantified by LC-MS/MS. Regarding lurbinectedin metabolites, only Metabolite 4 and Metabolite 6 were found at levels high enough to allow an accurate quantitation, with a percentage relative to lurbinectedin (*N*=3) of 0.9±0.7% and 0.4±0.2%, respectively. However, results showed that a sustained amount (2.1±0.7 ng-eq/mL) of ^{14}C-lurbinectedin-related radioactivity was retained in the pellets after plasma protein precipitation from 24 hours post-dose onwards that might produce a slight increase in exposure and half-life of total radioactivity vs. ^{14}C-lurbinectedin (Fig. 9).

With regards to excretion (*N*=3), only 49.9±4.0% of the radioactivity administered was recovered from the feces. The main lurbinectedin-related metabolite in feces was Metabolite 4 (2.9±0.3%) and its *N*-Desmethylated derivative (1.1±0.2%); other minor (≤0.6%) metabolites were identified as Metabolite 1, Metabolite 2 and Metabolite 6, as well as other oxidized derivatives, being these likely products of a chemical degradation rather than metabolism. Unchanged lurbinectedin only accounted for 0.4±0.1% of the dose administered to animals.

DMD Fast Forward. Published on January 18, 2022 as DOI: 10.1124/dmd.121.000668
This article has not been copyedited and formatted. The final version may differ from this version.

Owing to the low amount of ^{14}C-lurbinectedin-related radioactivity found in the urine, metabolic profiling was not attempted.

Mass Balance in Patients

Human mass balance studies with anticancer agents are performed in patients with advanced solid tumors who have exhausted therapeutic options (Beumer et al., 2006; Nijenhuis et al., 2016). The approach of performing these studies by recruiting patients with the same tumor type may offer some advantages (such as reduced variability or increased accuracy of estimated pharmacokinetic parameters), although the feasibility of the study may be hampered due to the difficulty of patient recruitment. In the human mass balance with lurbinectedin, no tumor type restrictions was applied because the pharmacokinetic variability of lurbinectedin cannot be explained by the tumor type (Fernandez-Teruel et al., 2019), as in most of the human mass balance studies (Beumer et al., 2006).

Near complete recovery of administered radioactivity (94.3±8.7%; *N*=6) was achieved within 500-hours post-dose, following a single mass dose of 4.29±0.23 mg of ^{14}C-lurbinectedin (radioactive dose of 74.28±8.62 µCi) administered as a 1-hour intravenous infusion.

Whole blood-to-plasma ratio of total ^{14}C-lurbinectedin-related radioactivity (as determined with mean $AUC_{0\text{-last}}$ values) was 0.7, being in agreement with the *in vitro* results that suggested a limited lurbinectedin distribution to blood (Fig. 6). The plasma t_{max} values for total ^{14}C-lurbinectedin-related radioactivity and lurbinectedin were similar (1.22±0.34 hour), the other main pharmacokinetic parameters were higher as compared to parent compound: C_{max} (1.4-fold: 154±88 ng-eq/mL vs. 108±46 ng/mL), $AUC_{0\text{-last}}$ (1.6-fold: 1438±1241 ng-eq·h/mL vs. 889±883 ng·h/mL), $AUC_{0\text{-}\infty}$ (1.9-fold: 1789±1555 ng-eq·h/mL vs. 962±961 ng·h/mL), $t_{1/2}$ (1.2-fold: 55±40 h vs. 47±14 h), CL (1.7-fold: 6.0±4.9 L/h vs. 10.2±7.4 L/h) and Vd_z (0.5-fold: 285±105 L vs. 598±366 L). The value of $AUC_{0\text{-last}}$ calculated for lurbinectedin was 66.6±27.5% of the corresponding value obtained for total ^{14}C-lurbinectedin-related radioactivity, therefore demonstrating that lurbinectedin is the main plasma circulating chemical entity (Fig. 7 C). Up to 10-hours after the end of infusion (Fig. 9B), 87.0±10.3% of the total ^{14}C-radioactivity in plasma can be attributed to lurbinectedin (70.2±10.9%) plus four metabolites (17.1±7.6%) among which, the main circulating metabolites were

DMD Fast Forward. Published on January 18, 2022 as DOI: 10.1124/dmd.121.000668
This article has not been copyedited and formatted. The final version may differ from this version.

Metabolite 4 (9.4±6.2% of total radioactivity; 14.3±10.4% of unchanged lurbinectedin) and Metabolite 6 (6.7±1.4% of total radioactivity; 10.4±2.2% of unchanged compound); other minor circulating metabolites were Metabolite 1 (0.6±0.3% of total radioactivity; 0.8±0.5% of unchanged lurbinectedin), Metabolite 2 (0.5±0.2% of total radioactivity; 0.8±0.3% of unchanged lurbinectedin) and Metabolite 7 (PM030779), which only was detected at concentrations below the lower limit of quantitation (0.1 ng/mL) (Fig. 9B).

Regarding excretion, the majority of radioactivity administered was found in feces (88.7±10.1%) (Fig. 8B), with minimal excretion in urine (5.6±2.0%) (Fig. 8C). In feces, the profiling of secreted metabolites was hampered by a very high inter-patient fecal excretion profile (likely owing to gastro-intestinal drug-induced disturbances, e.g. constipation) and a very low recovery of radioactivity (28.5%). Only traces (<0.2% of the administered radioactivity) of unchanged lurbinectedin were detected, although a large number of metabolites were found in feces, the more abundant (1.1% of the administered radioactivity) being Metabolite 4. In urine, only 5.6±2.0% of the administered radioactivity was recovered, having been quantified lurbinectedin and Metabolite 6 (1% each).

DMD Fast Forward. Published on January 18, 2022 as DOI: 10.1124/dmd.121.000668
This article has not been copyedited and formatted. The final version may differ from this version.

8. DISCUSSION

The results summarized in the present study, in which nonclinical species (rats and NHP) and patients received ^{14}C-lurbinectedin as a single intravenous administration, as well as results gathered from *in vitro* experiments also presented herein, provide a complete set of information about the pharmacokinetics, biotransformation and elimination of lurbinectedin and its metabolites.

In both nonclinical species and patients treated with ^{14}C-lurbinectedin, the highest concentration of total radioactivity was always recorded at the shortest sampling time, or immediately after the end of the infusion time (in patients). Thereafter, ^{14}C-related-lurbinectedin radioactivity quickly declined in a multi-exponential manner, followed by more prolonged distribution and terminal phases. In patients, the pharmacokinetic behavior of ^{14}C-related-lurbinectedin was similar to that seen in nonclinical species, and was characterized by a low-to-moderate systemic clearance, an extensive volume of distribution, and a long terminal half-life.

In nonclinical species and patients, total radioactivity values found in blood and plasma were numerically close consistently, regardless of the sampling time, these results being in agreement with the *in vitro* blood-to-plasma partitioning ratio calculated in rats, NHP and human samples, in which preferential distribution of lurbinectedin into cellular blood components, was not detected.

In vitro studies indicated that the CYP3A4/5-mediated metabolism of lurbinectedin is very intense in NHP and in humans, and to a less extent in rats. Following 10 minutes of incubation, 80 and 95% of compound was metabolized in human and NHP microsomes, respectively, although only a 30% was transformed in rat-derived microsomes. The microsomal-mediated biotransformation *N*-Desmethylation and/or aliphatic ring opening and/or the *O*-Desmethylation are the pathways involved in the metabolism of lurbinectedin. These *in vitro* results demonstrated that the aliphatic ring opening is a change that occurs only in NHP and human lurbinectedin microsomal-mediated metabolism. In the three species, similar amounts of the other metabolites were found, except the *O*-Desmethylated (as well as the *N*-, *O*-Desmethylated) and the aliphatic ring opening of the *N*-Desmethylated metabolites that were absent in the *in vitro* incubations with rat microsomes. These results suggest that the CYP3A4/5 equivalent isoform in the

DMD Fast Forward. Published on January 18, 2022 as DOI: 10.1124/dmd.121.000668
This article has not been copyedited and formatted. The final version may differ from this version.

rat is unable to act on the methylendioxy ring resulting, therefore, in the absence of this metabolic transformation or related, such as its *N*-demethylation, in rodents.

The *in vitro* results above described were reflected in the plasma metabolic profiling *in vivo* in which, the same systemic lurbinectedin-related metabolites are present in both NHP and patients. In the analysis of plasma samples generated in the mass balance study conducted in NHP, results demonstrated that the sum of the 5 components, lurbinectedin, pellets, rinses (quantified by liquid scintillation) and Metabolite 4 and Metabolite 6 (quantified by LC-MS/MS) gave a total concentration very similar to the total radioactivity measured in plasma (by liquid scintillation counting), resulting in overlapped concentration-time curves. Results showed that a sustained amount (2.1±0.1 ng-eq/mL) of ^{14}C-lurbinectedin-related radioactivity was retained in the pellets after plasma protein precipitation from 24 hours post-dose onwards. This consistent finding explained the increased exposure (expressed as $AUC_{0\text{-}144h}$) and half-life of total radioactivity vs. ^{14}C-lurbinectedin; however, similar values were determined for Vd_{ss} and CL. Regarding lurbinectedin metabolites, only Metabolite 4 and Metabolite 6 were found at levels high enough to allow an accurate quantitation, with a percentage relative to lurbinectedin of 0.9±0.7% and 0.4±0.2%, respectively. Similar results were obtained in patients. Systemic ^{14}C-lurbinectedin-related radioactivity may be mainly attributed to the unchanged compound and 17.1±7.6% to circulating metabolites namely, Metabolite 4 and Metabolite 6 and to a lesser extent, Metabolite 1 and Metabolite 2.

Notwithstanding, some quantitative differences were seen between NHP and patients. In NHP, the systemic exposure of lurbinectedin was lower than the corresponding values in patients, which is accepted as a common finding in antineoplastic-treated patients (DeGeorge et al., 1998). In particular, the recommended dose of lurbinectedin in patients is ca. 2-fold higher than the maximum tolerated dose in NHP that resulted in a higher systemic exposure to lurbinectedin, as well as to its main metabolite (Metabolite 4) in patients than in NHP.

Regardless of the study, the mean total radioactivity recovery successfully achieved an adequate (Roffey et al., 2007) cut-off (99.3±1.6% in rats, 82.0±1.6% in NHP and 94.3±8.7% in patients) for raising accurate conclusions. In rats, the radioactivity was principally recovered in the feces (cumulative 90.1±0.1% at 168 hours post-dose), with excretion via the urine occurring to a much smaller degree (3.0±0.6%). In bile cannulated animals, a mean biliary excretion of 49.9±11.2% of the administered dose

DMD Fast Forward. Published on January 18, 2022 as DOI: 10.1124/dmd.121.000668
This article has not been copyedited and formatted. The final version may differ from this version.

was found during the 0-72 hours period. Similar results were found in male NHP, with the cumulative (up to 168 hours post-dose) excreted radioactivity mainly found in feces; only 4.0±1.1% was found in urine. In agreement with these nonclinical results, in patients the excretion of radiolabeled material occurred predominantly through the feces, with only small amounts of radioactivity recovered from the urine. The metabolic profiling in feces (from NHP and patients) was hampered by the very low amount of radioactivity recovered during the extraction procedures that were tried (49.0±4.0% in NHP and 28.5% in patients), likely owing to the concomitant chemical interaction of ^{14}C-lurbinectedin, and/or its metabolites, and/or degradation products with matrix components, as well as gastro-intestinal drug-induced or condition-related (in patients) disturbances.

As already mentioned, lurbinectedin is a new synthetic ecteinascidin, chemical analog of trabectedin. Both compounds only differ because of the replacement of a tetrahydro β-carboline ring (in lurbinectedin) by a tetrahydroisoquinoline ring (in trabectedin) (He et al., 2019). Although the nonclinical evaluations carried out with both compounds demonstrated that the *in vitro* and *in vivo* antitumor activity resulted unaffected by these small structural changes (Romano et al., 2013), pharmacokinetic differences and decreased toxicity were recorded in patients, which allows higher dose intensities in lurbinectedin than in trabectedin. Thus, in phase I clinical studies, the recommended doses for the treatment of patients with solid tumors were determined to be 1.5 mg/m^2 and 4 mg/m^2 for trabectedin (van Kesteren et al., 2000; Taamma et al., 2001; Twelves et al., 2003; Chuk et al., 2012) and lurbinectedin (Elez et al., 2014), respectively. More importantly, at the recommended dose level, biochemical hepatic toxicity (increases in transaminases, alkaline phosphatase and/or hyperbilirubinemia) was more severe in trabectedin (Twelves et al., 2003) than in lurbinectedin treated patients, in whom only mild alkaline phosphatase and transaminase increases were recorded (Elez et al., 2014).

One possible explanation for the different safety profiles of trabectedin and lurbinectedin in patients could be that the metabolism of trabectedin involves the generation of an additional 1,2-cathecol from the 6-Hydroxy-7-Methoxy substitution in the dopamine ring (Vermeir et al., 2009). However, because of the dopamine ring replacement by a β-carboline in lurbinectedin´s structure, the above-described substitution is not feasible. The presence of this additional catechol group in a ring, which can interact with adjacent nuclear proteins and, that can be further oxidized to a

DMD Fast Forward. Published on January 18, 2022 as DOI: 10.1124/dmd.121.000668
This article has not been copyedited and formatted. The final version may differ from this version.

reactive quinone intermediate that is capable of adducting protein (McDonald and Rettie, 2007) and hence, may lead to the possibility of trabectedin-induced liver injury, owing to the local generation of this specific metabolite. As previously detailed, because of the structural differences between both compounds, this mechanism of inducing toxicity is unfeasible in lurbinectedin.

Taken all together, the *in vitro* and *in vivo* results demonstrated that lurbinectedin is mainly cleared by oxidative metabolism mediated by the CYP3A4/5 isoform. The higher metabolic similarities were found between NHP and human. In all the species analyzed, none of the metabolites produced were generated in a large amount as circulating metabolites. Rather, both unchanged lurbinectedin and related metabolites are directly eliminated, via biliary excretion, to feces, with only a minor contribution in the urine.

DMD Fast Forward. Published on January 18, 2022 as DOI: 10.1124/dmd.121.000668
This article has not been copyedited and formatted. The final version may differ from this version.

9. ACKNOWLEDGMENTS

The authors gratefully acknowledge the members of PharmaMar S.A. Organic Chemistry Laboratories for providing lurbinectedin, ^{14}C-lurbinectedin (coded as PM100567), deuterated lurbinectedin (coded as PM040038), as well as the reference standards for primary metabolites, namely, PM030036, PM01158, PM030047, and PM030779, and the impurity PM080323.

DMD Fast Forward. Published on January 18, 2022 as DOI: 10.1124/dmd.121.000668
This article has not been copyedited and formatted. The final version may differ from this version.

10. AUTHORSHIP CONTRIBUTION

Participated in research design:	Altares, van Andel, Lubomirov, Fudio, Rosing, Tibben, Nan-Offeringa, Schellens, Beijnen, Aviles
Conducted experiments:	Altares, van Andel, Márquez del Pino, Benedit, Tibben, Nan-Offeringa, Luepke
Contributed new reagents or analytic tools:	Altares, van Andel
Performed data analysis	Altares, van Andel, Lubomirov, Fudio, Rosing, Tibben, Nan-Offeringa, Francesch, Schellens, Beijnen, Aviles
Wrote or contributed to the writing of the manuscript:	Altares, van Andel, Lubomirov, Fudio, Rosing, Tibben, Nan-Offeringa, Francesch, Zeaiter, Cuevas, Schellens, Beijnen, Aviles

DMD Fast Forward. Published on January 18, 2022 as DOI: 10.1124/dmd.121.000668
This article has not been copyedited and formatted. The final version may differ from this version.

11. REFERENCES

Altares R, Marquez del Pino FM, Benedit G, Guillen MJ, Cuevas C, Perez de la Cruz MA, and Aviles P (2019) Development of a New Method for the Quantitation of Metabolites in the Absence of Chemically Synthetized Authentic Standards. *J Pharm Biomed Anal* **169:**70-74.

Belgiovine C, Bello E, Liguori M, Craparotta I, Mannarino L, Paracchini L, Beltrame L, Marchini S, Galmarini CM, Mantovani A, Frapolli R, Allavena P, and D'Incalci M (2017) Lurbinectedin reduces tumour-associated macrophages and the inflammatory tumour microenvironment in preclinical models. *Br J Cancer* **117:**628-638.

Beumer JH, Beijnen JH, and Schellens JH (2006) Mass balance studies, with a focus on anticancer drugs. *Clin Pharmacokinet* **45:**33-58.

Cespedes MV, Guillen MJ, Lopez-Casas PP, Sarno F, Gallardo A, Alamo P, Cuevas C, Hidalgo M, Galmarini CM, Allavena P, Aviles P, and Mangues R (2016) Lurbinectedin induces depletion of tumor-associated macrophages, an essential component of its in vivo synergism with gemcitabine, in pancreatic adenocarcinoma mouse models. *Dis Model Mech* **9:**1461-1471.

Chuk MK, Aikin A, Whitcomb T, Widemann BC, Zannikos P, Bayever E, Balis FM, and Fox E (2012) A phase I trial and pharmacokinetic study of a 24-hour infusion of trabectedin (Yondelis(R), ET-743) in children and adolescents with relapsed or refractory solid tumors. *Pediatr Blood Cancer* **59:**865-869.

DeGeorge JJ, Ahn CH, Andrews PA, Brower ME, Giorgio DW, Goheer MA, Lee-Ham DY, McGuinn WD, Schmidt W, Sun CJ, and Tripathi SC (1998) Regulatory considerations for preclinical development of anticancer drugs. *Cancer Chemother Pharmacol* **41:**173-185.

Di Giandomenico S, Frapolli R, Bello E, Uboldi S, Licandro SA, Marchini S, Beltrame L, Brich S, Mauro V, Tamborini E, Pilotti S, Casali PG, Grosso F, Sanfilippo R, Gronchi A, Mantovani R, Gatta R, Galmarini CM, Sousa-Faro JM, and D'Incalci M (2014) Mode of action of trabectedin in myxoid liposarcomas. *Oncogene* **33:**5201-5210.

Elez ME, Tabernero J, Geary D, Macarulla T, Kang SP, Kahatt C, Pita AS, Teruel CF, Siguero M, Cullell-Young M, Szyldergemajn S, and Ratain MJ (2014) First-in-human phase I study of Lurbinectedin (PM01183) in patients with advanced solid tumors. *Clin Cancer Res* **20:**2205-2214.

Fernandez-Teruel C, Gonzalez I, Troconiz IF, Lubomirov R, Soto A, and Fudio S (2019) Population-Pharmacokinetic and Covariate Analysis of Lurbinectedin (PM01183), a New RNA Polymerase II Inhibitor, in Pooled Phase I/II Trials in Patients with Cancer. *Clin Pharmacokinet* **58:**363-374.

Harlow ML, Maloney N, Roland J, Guillen Navarro MJ, Easton MK, Kitchen-Goosen SM, Boguslawski EA, Madaj ZB, Johnson BK, Bowman MJ, D'Incalci M, Winn ME, Turner L, Hostetter G, Galmarini CM, Aviles PM, and Grohar PJ (2016) Lurbinectedin Inactivates the Ewing Sarcoma Oncoprotein EWS-FLI1 by Redistributing It within the Nucleus. *Cancer Res* **76:**6657-6668.

He W, Zhang Z, and Ma D (2019) A Scalable Total Synthesis of the Antitumor Agents Et-743 and Lurbinectedin. *Angew Chem Int Ed Engl* **58:**3972-3975.

Leal JF, Martinez-Diez M, Garcia-Hernandez V, Moneo V, Domingo A, Bueren-Calabuig JA, Negri A, Gago F, Guillen-Navarro MJ, Aviles P, Cuevas C, Garcia-Fernandez LF, and Galmarini CM (2010) PM01183, a new DNA minor groove covalent binder with potent in vitro and in vivo anti-tumour activity. *Br J Pharmacol* **161:**1099-1110.

McDonald MG and Rettie AE (2007) Sequential metabolism and bioactivation of the hepatotoxin benzbromarone: formation of glutathione adducts from a catechol intermediate. *Chem Res Toxicol* **20:**1833-1842.

Nijenhuis CM, Schellens JH, and Beijnen JH (2016) Regulatory aspects of human radiolabeled mass balance studies in oncology: concise review. *Drug Metab Rev* **48:**266-280.

Oliveira EJ and Watson DG (2000) Liquid chromatography-mass spectrometry in the study of the metabolism of drugs and other xenobiotics. *Biomed Chromatogr* **14:**351-372.

Roffey SJ, Obach RS, Gedge JI, and Smith DA (2007) What is the objective of the mass balance study? A retrospective analysis of data in animal and human excretion studies employing radiolabeled drugs. *Drug Metab Rev* **39:**17-43.

Romano M, Frapolli R, Zangarini M, Bello E, Porcu L, Galmarini CM, Garcia-Fernandez LF, Cuevas C, Allavena P, Erba E, and D'Incalci M (2013) Comparison of in vitro and in vivo biological effects of trabectedin, lurbinectedin (PM01183) and Zalypsis(R) (PM00104). *Int J Cancer* **133:**2024-2033.

Santamaria Nunez G, Robles CM, Giraudon C, Martinez-Leal JF, Compe E, Coin F, Aviles P, Galmarini CM, and Egly JM (2016) Lurbinectedin Specifically Triggers the Degradation of Phosphorylated RNA Polymerase II and the Formation of DNA Breaks in Cancer Cells. *Mol Cancer Ther* **15:**2399-2412.

Taamma A, Misset JL, Riofrio M, Guzman C, Brain E, Lopez Lazaro L, Rosing H, Jimeno JM, and Cvitkovic E (2001) Phase I and pharmacokinetic study of ecteinascidin-743, a new marine compound, administered as a 24-hour continuous infusion in patients with solid tumors. *J Clin Oncol* **19:**1256-1265.

Takahashi R, Mabuchi S, Kawano M, Sasano T, Matsumoto Y, Kuroda H, Kozasa K, Hashimoto K, Sawada K, and Kimura T (2016) Preclinical Investigations of PM01183 (Lurbinectedin) as a Single Agent or in Combination with Other Anticancer Agents for Clear Cell Carcinoma of the Ovary. *PLoS One* **11:**e0151050.

Trigo J, Subbiah V, Besse B, Moreno V, Lopez R, Sala MA, Peters S, Ponce S, Fernandez C, Alfaro V, Gomez J, Kahatt C, Zeaiter A, Zaman K, Boni V, Arrondeau J, Martinez M, Delord JP, Awada A, Kristeleit R, Olmedo ME, Wannesson L, Valdivia J, Rubio MJ, Anton A, Sarantopoulos J, Chawla SP, Mosquera-Martinez J, D'Arcangelo M, Santoro A, Villalobos VM, Sands J, and Paz-Ares L (2020) Lurbinectedin as second-line treatment for patients with small-cell lung cancer: a single-arm, open-label, phase 2 basket trial. *Lancet Oncol* **21:**645-654.

Twelves C, Hoekman K, Bowman A, Vermorken JB, Anthoney A, Smyth J, van Kesteren C, Beijnen JH, Uiters J, Wanders J, Gomez J, Guzmán C, Jimeno J, and Hanauske A (2003) Phase I and pharmacokinetic study of Yondelis (Ecteinascidin-743; ET-743) administered as an infusion over 1 h or 3 h every 21 days in patients with solid tumours. *European journal of cancer (Oxford, England : 1990)* **39:**1842-1851.

van Andel L, Rosing H, Lubomirov R, Aviles P, Fudio S, Tibben MM, Nan-Offeringa L, Schellens JHM, and Beijnen JH (2018) Development and validation of a liquid chromatography-tandem mass spectrometry assay for the quantification of lurbinectedin in human plasma and urine. *J Pharm Biomed Anal* **158:**160-165.

van Kesteren C, Cvitkovic E, Taamma A, López-Lázaro L, Jimeno JM, Guzman C, Mathôt RAA, Schellens JHM, Misset J-L, Brain E, Hillebrand MJX, Rosing H, and Beijnen JH (2000) Pharmacokinetics and Pharmacodynamics of the Novel Marine-derived Anticancer Agent Ecteinascidin 743 in a Phase I Dose-finding Study. *Clin Cancer Res* **6:**4725-4732.

Vermeir M, Hemeryck A, Cuyckens F, Francesch A, Bockx M, Van Houdt J, Steemans K, Mannens G, Aviles P, and De Coster R (2009) In vitro studies on the metabolism of trabectedin (YONDELIS) in monkey and man, including human CYP reaction phenotyping. *Biochem Pharmacol* **77:**1642-1654.

Vidal A, Munoz C, Guillen MJ, Moreto J, Puertas S, Martinez-Iniesta M, Figueras A, Padulles L, Garcia-Rodriguez FJ, Berdiel-Acer M, Pujana MA, Salazar R, Gil-Martin M, Marti L, Ponce J, Mollevi DG, Capella G, Condom E, Vinals F, Huertas D, Cuevas C, Esteller M, Aviles P, and Villanueva A (2012) Lurbinectedin (PM01183), a new DNA minor groove

binder, inhibits growth of orthotopic primary graft of cisplatin-resistant epithelial ovarian cancer. *Clin Cancer Res* **18:**5399-5411.

12. FOOTNOTES

Financial disclosure: Aviles, Altares, Fudio, Lubomirov, Marquez del Pino, Benedit, Luepke, Francesch, Zeaiter and Cuevas are PharmaMar S.A. employees or PharmaMar S.A. shareholders or both.

The Netherlands Cancer Institute (in)directly received financial support from PharmaMar to execute the study.

DMD Fast Forward. Published on January 18, 2022 as DOI: 10.1124/dmd.121.000668
This article has not been copyedited and formatted. The final version may differ from this version.

LEGENDS FOR FIGURES

Figure 1. Chemical structure of lurbinectedin. The site for one ^{14}C substitution was C4; the four ^{2}H substitutions in the internal standard were located at C3 and C4.

Figure 2. Representative reconstructed radio-chromatograms following 10-min incubations of ^{14}C-lurbinectedin with NADPH-activated liver microsomes from (A) both genders pooled human; (B) male NHP; (C) female NHP; (D) male Sprague-Dawley rat; and, (E) female Sprague-Dawley rat.
Dotted line: change of component B (acetonitrile, 0.1 % formic acid) in the gradient.
Metabolites coding: M1 or Metabolite 1, *N*-Desmethyl-6-Hydroxy-lurbinectedin; M2 or Metabolite 2, 6-Hydroxy-lurbinectedin; M4 or Metabolite 4, 1',3'-Desmethylene-lurbinectedin; M6 or Metabolite 6, *N*-Desmethyl-lurbinectedin.

Figure 3. Mass spectrometric fragmentation pattern of lurbinectedin.

Figure 4. MS/MS spectra of (A) lurbinectedin; (B) Metabolite 1 (PM030036); (C) Metabolite 2 (PM01158); (D) Metabolite 4; and (E) Metabolite 6 (PM030047).

Figure 5. *In vitro* metabolic pathway of lurbinectedin in liver microsomes of nonclinical species (rat and NHP) and human. Dotted arrows represent potential redundant metabolism. Bold arrows indicate major human and NHP metabolites.

Figure 6. Effect of CYP (between brackets) isoform-selective chemical inhibitors on the transformation of lurbinectedin (200 nM; 157 ng/mL) in pooled human liver microsomes; (mean, *N*=3).

Figure 7. Representative concentration-time curves of total radioactivity in plasma (solid symbol) and blood (open symbol) following a single intravenous dose of ^{14}C-lurbinectedin in (A) rat (mean, *N*=3): at 1.2 mg/m^2 (male) and 0.6 mg/m^2 (female); (B) NHP (mean±SD, *N*=3; male): at 1.7 mg/m^2; and, (C) patients (mean±SD; *N*=6; both genders: 5 males, 1 female): at 5 mg flat dose (ca. 2.3 mg/m^2); mean concentration of lurbinectedin in plasma (as ng/mL) is also presented (grey symbol).

Figure 8. Cumulative radioactivity recovered from feces and urine after a single i.v. administration of ^{14}C-lurbinectedin: (A) bolus dose (1.7 mg/m^2) to male NHP (*N*=3); (B) 1-hour i.v. infusion dose (5 mg flat dose; ca. 2.3 mg/m^2) to patients (*N*=6).

Figure 9. Representative concentration-time curves: (Top) of total radioactivity, lurbinectedin, Metabolite 4 and Metabolite 6, as well as pellet and rinse obtained in

DMD Fast Forward. Published on January 18, 2022 as DOI: 10.1124/dmd.121.000668
This article has not been copyedited and formatted. The final version may differ from this version.

plasma of male NHP (mean±SD; *N*=3) after a single i.v. bolus dose at 1.7 mg/m^2 (0.142 mg/kg) of ^{14}C-lurbinectedin. (Bottom): of total radioactivity, lurbinectedin, Metabolite 1, Metabolite 2, Metabolite 4 and Metabolite 6 in plasma of patients (mean±SD; *N*=6) after 1-hour i.v. infusion dose (5 mg flat dose; ca. 2.3 mg/m^2) of ^{14}C-lurbinectedin up to 10 hours after the infusion end.

DMD Fast Forward. Published on January 18, 2022 as DOI: 10.1124/dmd.121.000668
This article has not been copyedited and formatted. The final version may differ from this version.

TABLES

Table 1

					Liver Microsomes from:				
					Human	NHP		Rat	
Compound	**Code**	**Metabolic Step**	**RT (min)[a]**	**RRT**	**M/F**	**M**	**F**	**M**	**F**
^{14}C-lurbinectedin	**PM100567**	-	14.3	-	17.8±5.8	5.9±0.1	5.2±1.2	65.1±8.9	76.9±11.6
Metabolite 1	**PM030036**	*N*-,*O*-Desmethylation	8.7	0.61	8.2±0.5	4.3±0.3	4.8±0.3	-	-
Metabolite 2	**PM01158**	*O*-Desmethylation	9.0	0.63	3.8±0.1	4.1±0.1	4.7±0.3	-	-
Metabolite 3	**-**	*Aliphatic ring opening of Metabolite 6*	*10.4*	*0.73*	*4.9±0.5*	*5.7±0.6*	*7.6±0.6*	-	-
Metabolite 4	**-**	Aliphatic ring opening	11.0	0.77	16.3±0.2	28.3±2.6	25.1±2.7	3.3±0.2	1.9±0.6
Metabolite 5	**-**	*Oxidation of Metabolite 6*	*12.9*	*0.90*	*13.2±1.1*	*12.7±0.7*	*12.6±1.3*	*12.3±0.8*	*3.5±0.9*
Metabolite 6	**PM030047**	*N*-Desmethylation	13.8	0.96	19.1±3.0	11.1±1.3	12.2±1.2	10.3±1.0	16.6±3.0
		Post-column recovery (%)			**83.3±11.1**	**72.1±5.8**	**72.2±7.5**	**91.0±10.9**	**98.8±16.1**

NHP, nonhuman primate.
RT, retention time.
RRT, relative retention time.
M, male; F, female.
Italics denote metabolites that were produced from primary lurbinectedin-related metabolites.

[a]Time of the collected fraction with the highest content in radioactivity.

Table 1. Comparative quantitative *in vitro* metabolism of ^{14}C-lurbinectedin in microsomes from nonclinical species (both genders) and human (pooled) following 10 min of incubation.

DMD Fast Forward. Published on January 18, 2022 as DOI: 10.1124/dmd.121.000668
This article has not been copyedited and formatted. The final version may differ from this version.

Table 2

	Intact rats (0-168 hours)		Bile Duct-cannulated (0-72 hours)	
	Male	**Female**	**Male**	**Female**
Urine	3.4±1.4	2.6±0.5	NA	NA
Feces	91.0±2.1	91.2±1.7	9.4[a]	10.8[a]
Bile	NA	NA	57.8±4.9	41.9±1.7
Cage wash	0.4±0.4	0.4±0.4	NA	NA
Carcass	3.2±0.2	6.2±0.8	18.6±3.0	34.5±3.6
Total recovery	98.1±1.1	100.4±1.7	85.9[b]	87.3[b]

NA, not applicable.

[a] Pooled feces.

[b] Standard deviation not calculated: not individual values for feces were available.

Note: divide by 6 to determine the dose in mg/kg.

Table 2. Cumulative excretion and mass balance (as % of the radioactivity dosed) after a single intravenous bolus dose of ^{14}C-lurbinectedin at 1.2 and 0.6 mg/m^2 in male and female Sprague-Dawley rats (mean±SD; *N*=3/gender), respectively.

DMD Fast Forward. Published on January 18, 2022 as DOI: 10.1124/dmd.121.000668
This article has not been copyedited and formatted. The final version may differ from this version.

DMD Fast Forward. Published on January 18, 2022 as DOI: 10.1124/dmd.121.000668
This article has not been copyedited and formatted. The final version may differ from this version.

Figure 1

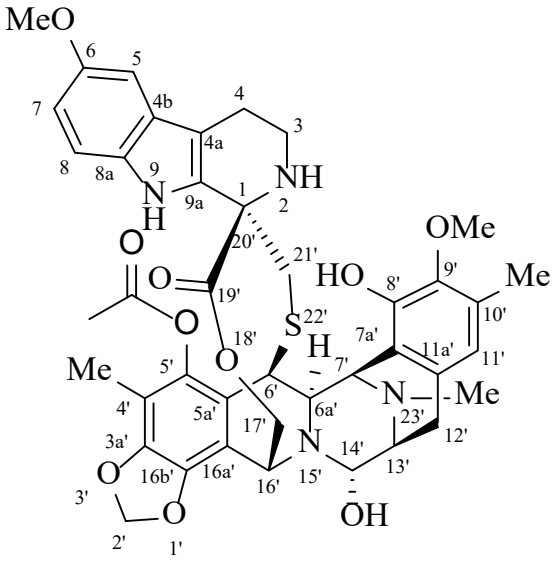

Figure 2

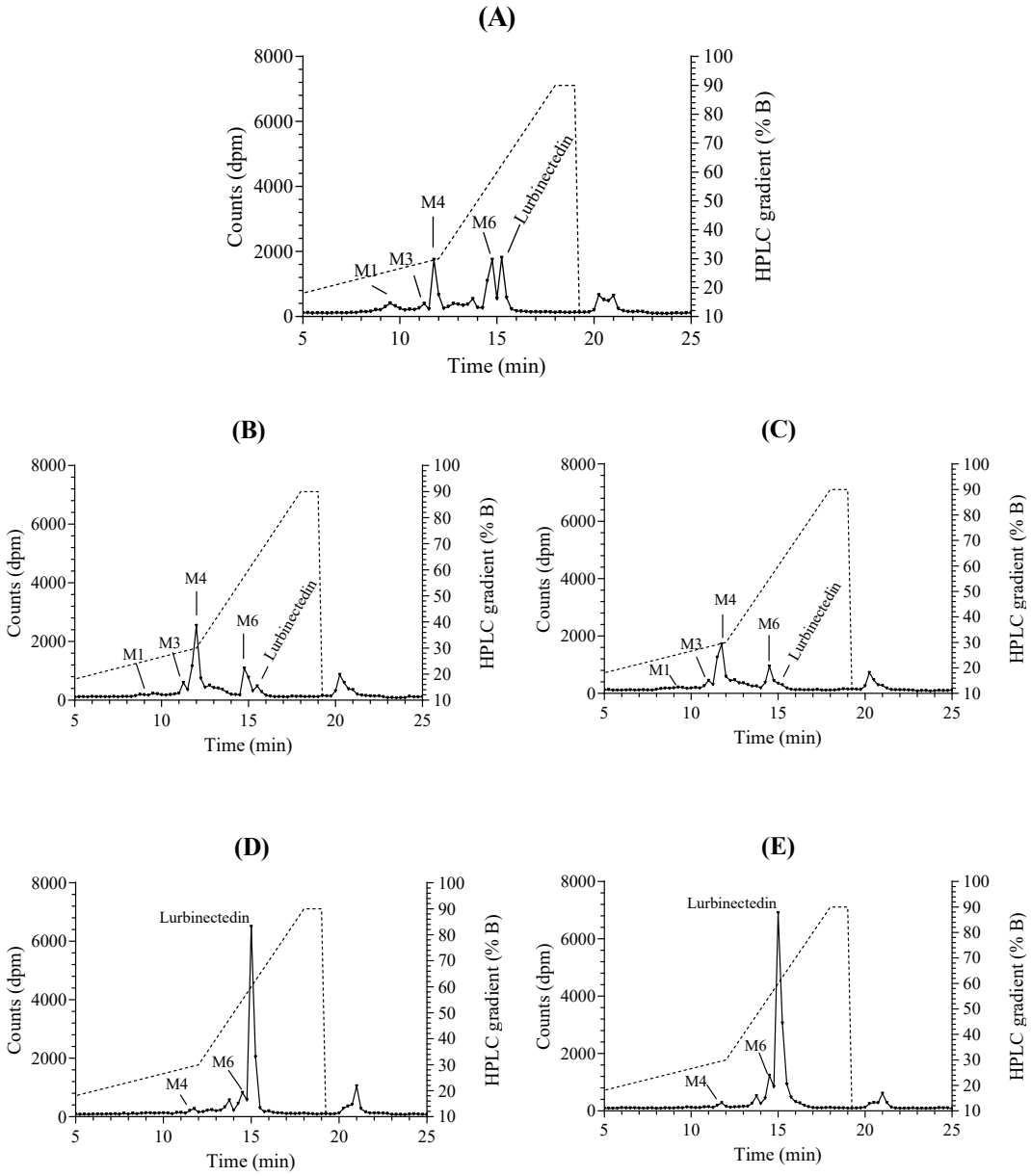

Figure 3

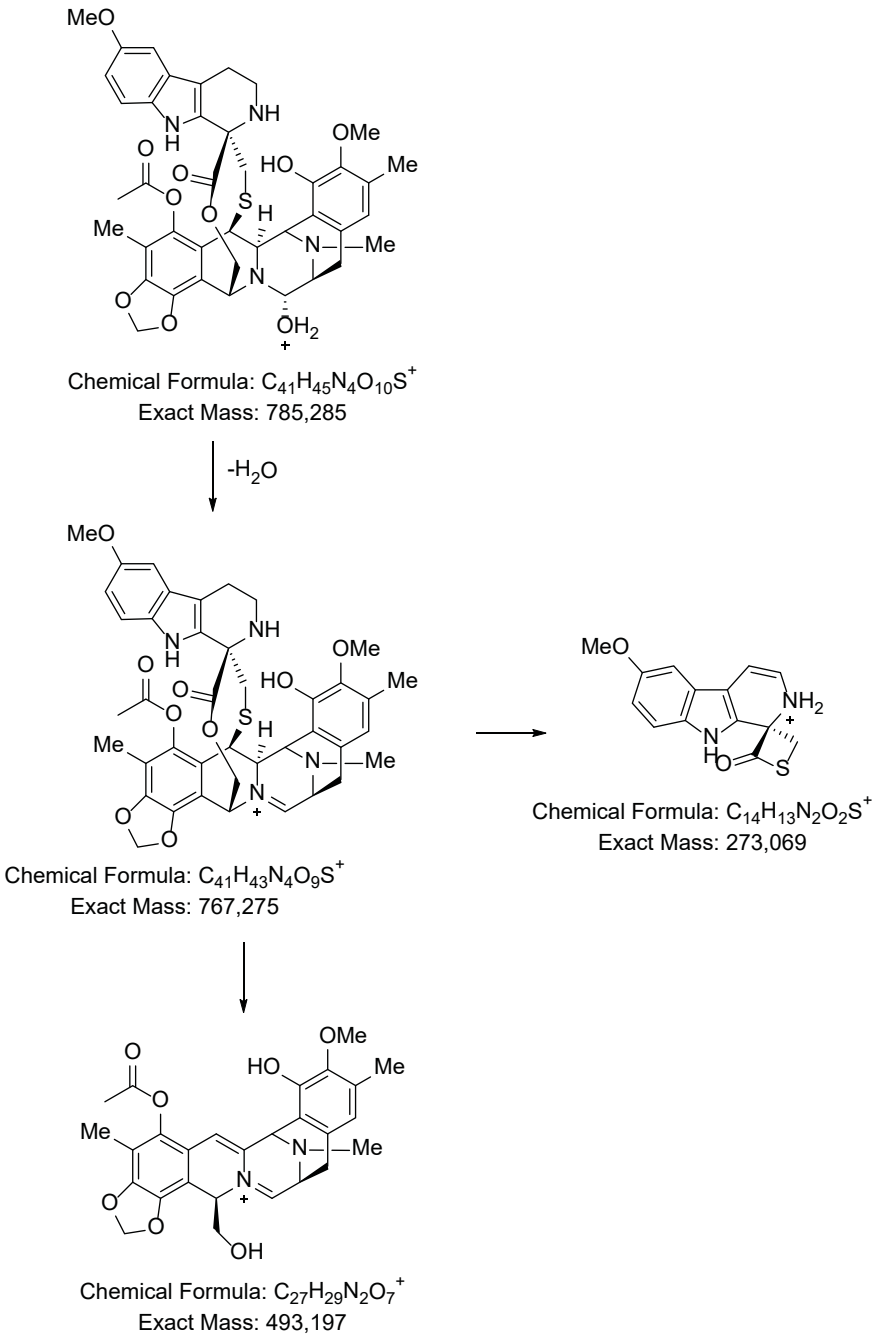

Figure 4

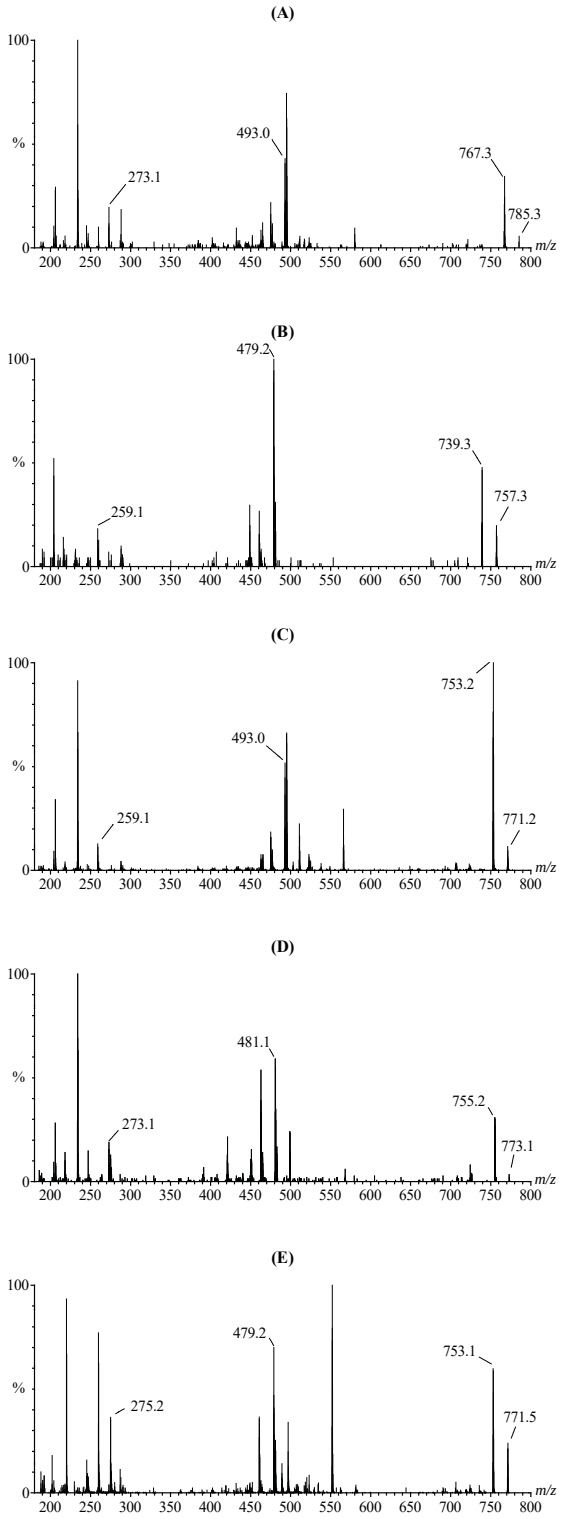

Figure 5

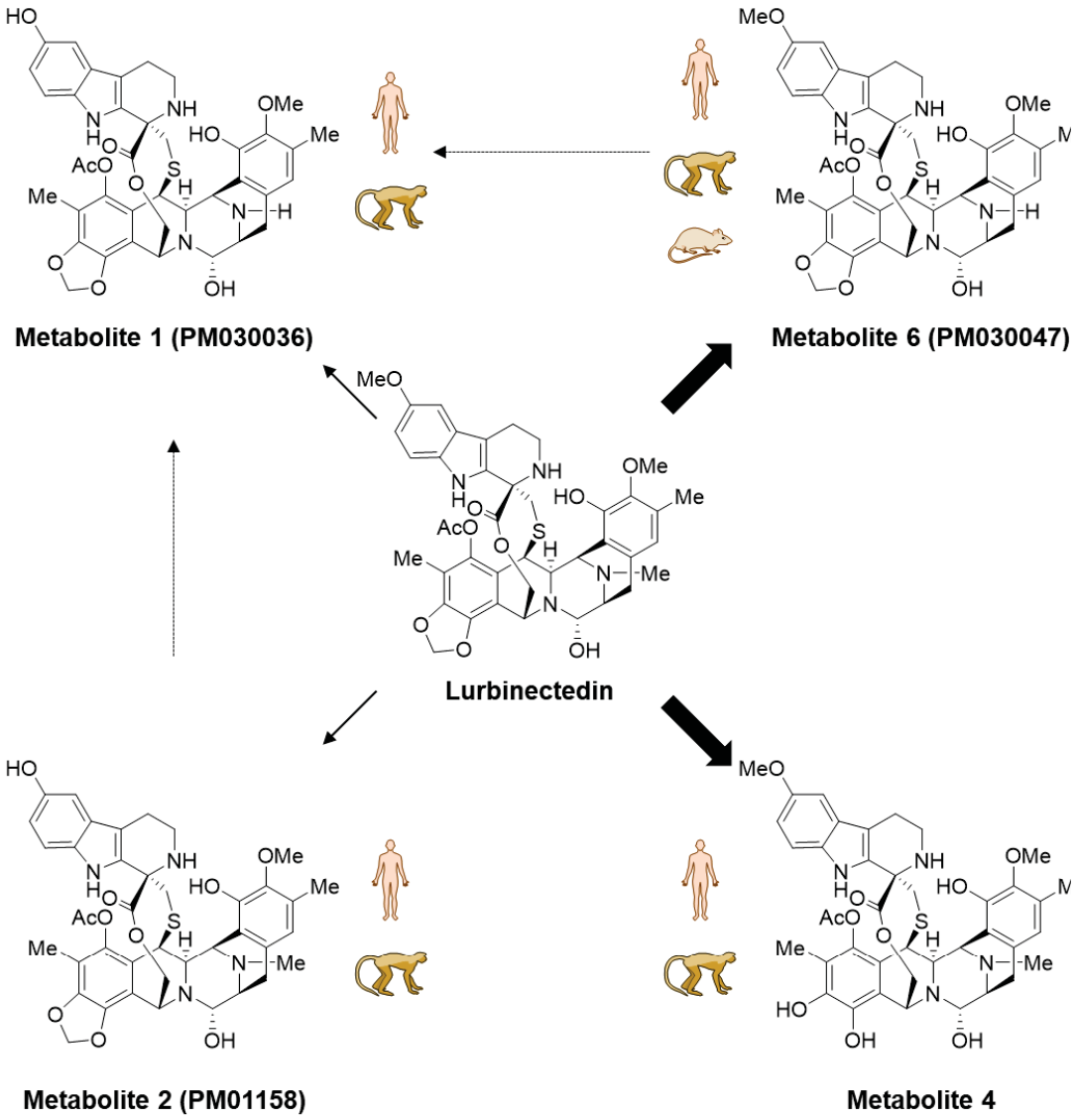

Figure 6

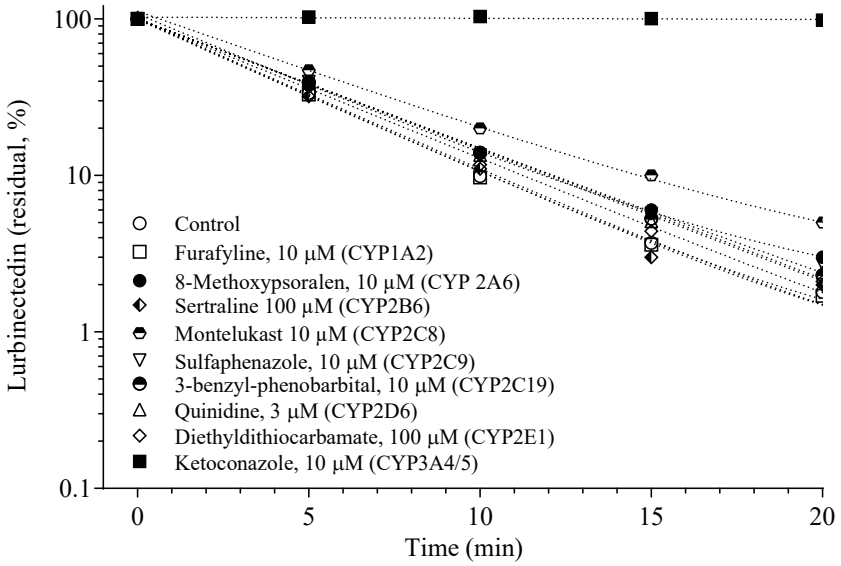

DMD Fast Forward. Published on January 18, 2022 as DOI: 10.1124/dmd.121.000668
This article has not been copyedited and formatted. The final version may differ from this version.

Figure 7

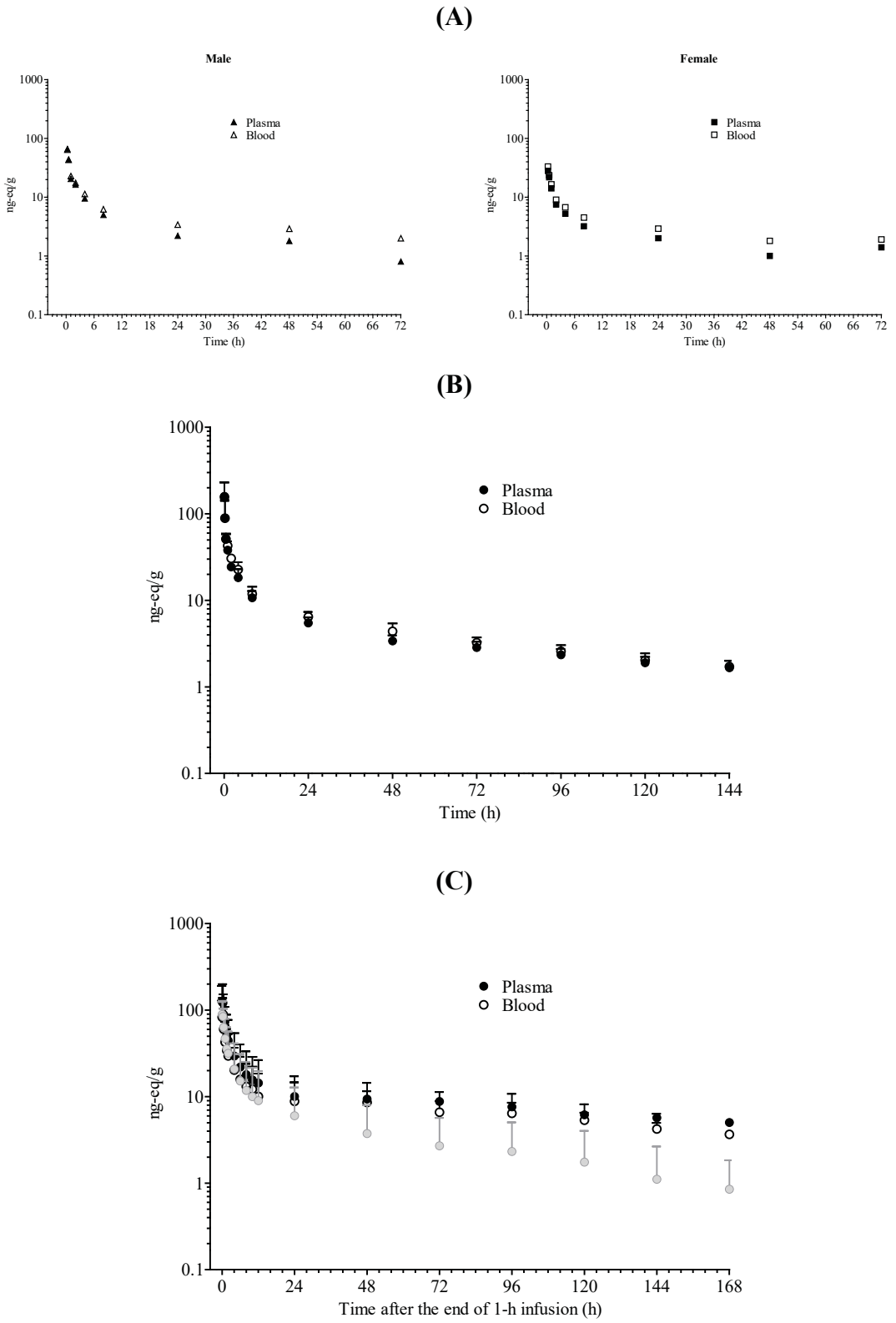

Figure 8

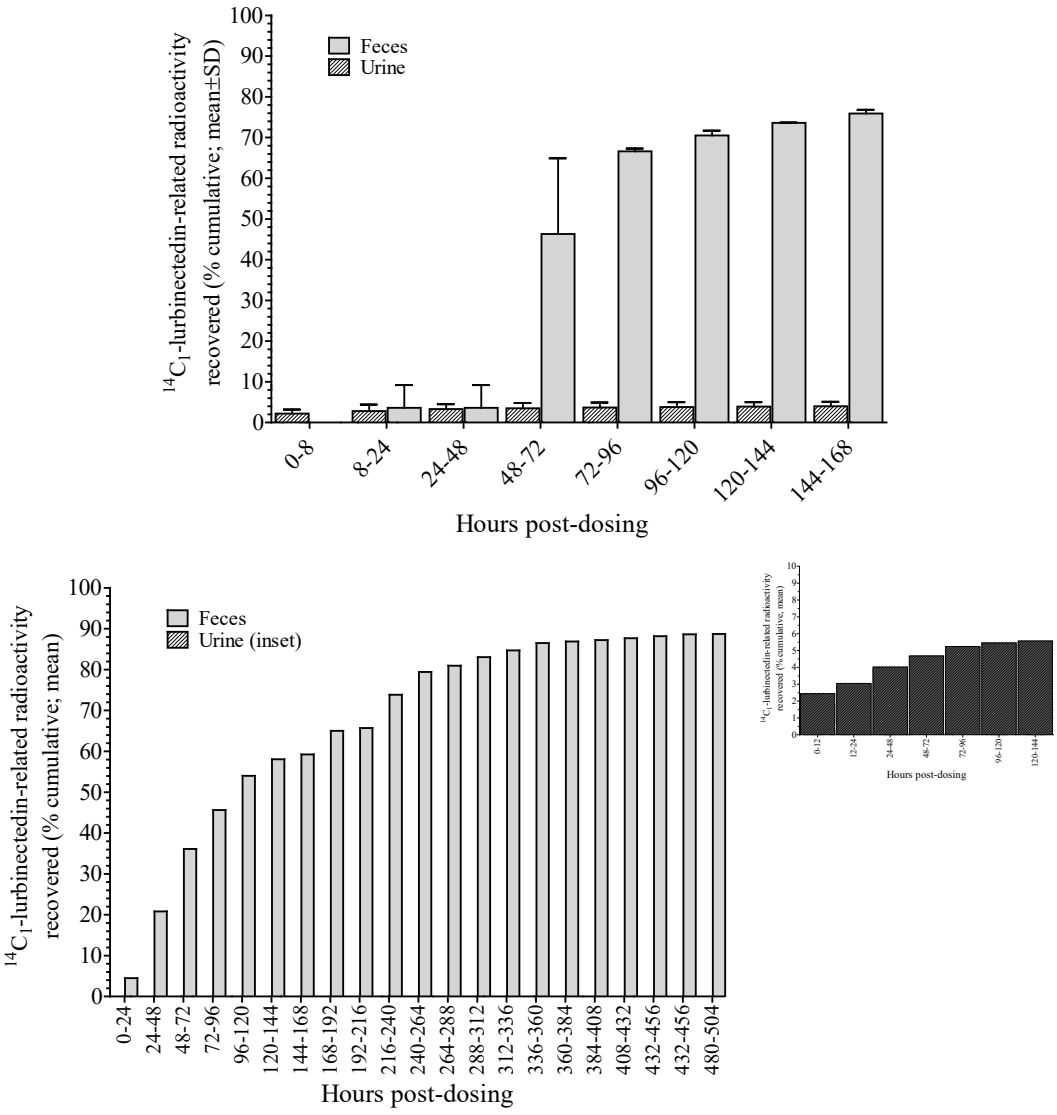

Figure 9